

Chromatic aberration control with liquid crystal spatial phase modulators

JOSE L. MARTINEZ,^{1,2} ENRIQUE J. FERNANDEZ,^{1,*} PEDRO M. PRIETO,¹ AND PABLO ARTAL¹

¹*Instituto de Investigación en Óptica y Nanofísica, Laboratorio de Óptica, Universidad de Murcia, Edificio 34, Campus de Espinardo, 30100 Murcia, Spain*

²*Departamento de Ciencia de Materiales, Óptica y Tecnología Electrónica, Universidad Miguel Hernández de Elche, 03202 Elche, Spain*

*enriquej@um.es

Abstract: The chromatic behavior of diffractive optical elements, exhibiting 2π -wrapped phase profiles, implemented into liquid crystal spatial light modulators (LC-SLM) is described. A wrapped phase map is only equivalent to the original continuous profile for the design wavelength while at other wavelengths there are unwanted phase jumps and the profile does not correspond to a pure defocus. For those conditions the wrapped profile behaves as a multiple order lens (multi-focal lens). The optical power dispersion for each order is linearly proportional to the wavelength, while the energy of each order depends on the design wavelength and the material dispersion. For practical purposes, for most of the visible range only first order (main defocus) is relevant but two other orders may also be considered depending on the actual PSF of the system. As an application, we demonstrate that the longitudinal chromatic aberration of the eye can be compensated by the diffractive lens dispersion when the appropriate defocus is programmed into the SLM.

© 2017 Optical Society of America

OCIS codes: (120.5060) Phase modulation; (110.1080) Active or adaptive optics; (230.3720) Liquid-crystal devices; (330.0330) Vision, color, and visual optics.

References and links

1. P. M. Prieto, E. J. Fernández, S. Manzanera, and P. Artal, "Adaptive optics with a programmable phase modulator: applications in the human eye," *Opt. Express* **12**(17), 4059–4071 (2004).
2. E. J. Fernández, P. M. Prieto, and P. Artal, "Wave-aberration control with a liquid crystal on silicon (LCOS) spatial phase modulator," *Opt. Express* **17**(13), 11013–11025 (2009).
3. E. J. Fernández, P. M. Prieto, and P. Artal, "Binocular adaptive optics visual," *Opt. Lett.* **34**(17), 2628–2630 (2009).
4. J. Albero, P. García-Martínez, J. L. Martínez, and I. Moreno, "Second order diffractive optical elements in a spatial light modulator with large phase dynamic range," *Opt. Lasers Eng.* **51**(2), 111–115 (2013).
5. V. Calero, P. García-Martínez, J. Albero, M. M. Sánchez López, and I. Moreno, "Liquid crystal spatial light modulator with very large phase modulation operating in high harmonic orders," *Opt. Lett.* **38**(22), 4663–4666 (2015).
6. D. Mas, J. Espinosa, J. Perez, and C. Illueca, "Three dimensional analysis of chromatic aberration in diffractive elements with extended depth of focus," *Opt. Express* **15**(26), 17842–17854 (2007).
7. P. Wang, N. Mohammad, and R. Menon, "Chromatic-aberration-corrected diffractive lenses for ultra-broadband focusing," *Sci. Rep.* **6**(1), 21545 (2016).
8. I. Moreno, C. Iemmi, A. Márquez, J. Campos, and M. J. Yzuel, "Modulation light efficiency of diffractive lenses displayed in a restricted phase-mostly modulation display," *Appl. Opt.* **43**(34), 6278–6284 (2004).
9. I. Moreno, C. Iemmi, A. Márquez, J. Campos, and M. J. Yzuel, "Modulation light efficiency of spatial light modulators," *Proceedings of IEEE Conference 10th Euro-American Workshop on Information Optics (IEEE, 2011)*, pp. 1–4.
10. D. W. Sweeney and G. E. Sommagren, "Harmonic diffractive lenses," *Appl. Opt.* **34**(14), 2469–2475 (1995).
11. D. M. Cottrell, J. A. Davis, T. R. Hedman, and R. A. Lilly, "Multiple imaging phase-encoded optical elements written as programmable spatial light modulators," *Appl. Opt.* **29**(17), 2505–2509 (1990).
12. J. L. M. Fuentes, E. J. Fernández, P. M. Prieto, and P. Artal, "Interferometric method for phase calibration in liquid crystal spatial light modulators using a self-generated diffraction-grating," *Opt. Express* **24**(13), 14159–14171 (2016).
13. D. A. Atchinson and G. Smith, "Chromatic dispersions of the ocular media of human eyes," *J. Opt. Soc. Am. A* **22**(1), 29–37 (2005).

1. Introduction

The use of liquid crystal spatial light modulators (LC-SLM) for ocular aberration correction and manipulation has been explored in previous works [1–3]. Since LC-SLMs typically provide a restricted phase modulation range, these devices are mainly operated under monochromatic light sources for which the proper phase modulation range (0 to 2π) was achieved.

LC-SLM exhibiting wide phase modulation also open the possibility for further chromatic control. In a previous work [4], the use of LC-SLM devices with extended phase range, i.e., from 0 to 4π , was showed for diminishing artifacts like fringing effects and pointed out the possibility of exploiting this fact to reduce chromatic aberrations. Further, inverted chromatic dispersion for a blazed diffraction grating was also reported [5] by using a very high phase modulation depth SLM which was designed for infrared and operated under visible light. A theoretical chromatic study of other elements, such as axicons or light swords [6], has also been reported in literature by means of diffraction integrals. This study explored the feasibility of creating achromatic axicons elements by controlling the design parameters. Even complex profile design techniques for creating zero dispersion diffractive lenses have recently been reported [7]. A useful tool for describing the response of general diffractive optical elements and particularly Fresnel diffractive lenses in devices with limited phase response was reported elsewhere [8,9]. That model was devised to describe the effects of non-ideal phase modulation profiles over the diffraction response of the lenses by means of a Fourier series theory. Those non-ideal profiles were meaningful in current devices, which offered limited phase response or even non-linear and coupled amplitude-phase response. Such approach could be seen less useful regarding actual LC-SLM devices, which offer almost perfect linear phase-only response, ranging from 0 to 2π or even greater multiples of 2π . Nonetheless, if such devices implement a properly codified lens at a given wavelength but it is illuminated with polychromatic light, the same model could also be applied to describe the chromatic behavior of the given lens.

Although there is a related analysis performed in the context of etched diffractive lenses [10], in this work we concentrated in practical chromatic aberration correction, providing an example of application for the optics of the human eye.

The aim of this work is to provide a model for understanding of the chromatic behavior of diffractive optical elements obtained by 2π -wrapping for a reference wavelength. As an application, the interaction of the eye's chromatic aberration with a lens generated by an LC-SLM is studied using the proposed formalism.

2. Theory and modeling

LC-SLM devices can implement diffractive optical elements which can be regarded as thin optical elements, where the minimum period in the encoded phase or amplitude is significantly larger than one or several of the employed wavelengths. Consequently, the emerging fields can be calculated by multiplying the incoming field by the programmed phase-only or amplitude transmittance or reflectance of the device. Under these conditions, the scalar diffraction theory can be applied to study the response of the device corresponding to such elements.

A condition to generate a given phase with the LC-SLM is that pixel size must be small enough to conform to the Nyquist frequency sampling theorem [11].

Figure 1 compares a continuous phase map that corresponds to a refractive element, in this case a spherical lens, and the discontinuous diffractive profile obtained by 2π -wrapping. Both profiles are optically equivalent when the design wavelength λ_0 is used. Since SLMs have no continuity constrains, they can reproduce the phase jumps typical of wrapped profiles, significantly increasing the effective stroke of the device, which now depends on

spatial resolution more than on optical path depth. However, for a different wavelength, $\lambda \neq \lambda_0$, these two phase-maps are no longer equivalent.

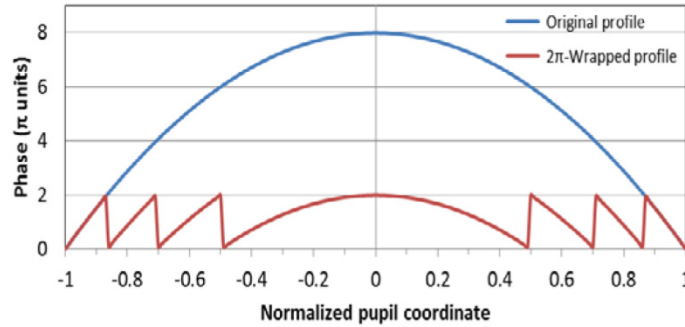


Fig. 1. Conceptual scheme comparing the phase profiles of a refractive element (pure defocus) and its equivalent diffractive element obtained by phase wrapping at design wavelength λ_0 .

Once calibrated and linearized [12] for wavelength, λ_0 , each LC-SLM pixel can be driven to regularly vary its refractive index inside a range, $\Delta n(\lambda_0)$, between two fixed values, in order to introduce phase values uniformly ranging from 0 to 2π . The set of phase values can be expressed as:

$$\varphi(\lambda_0) = \frac{2\pi}{\lambda_0} \Delta n(\lambda_0) \cdot d \cdot g, \quad (1)$$

where d is the liquid crystal thickness, and g represents the phase level index and takes uniformly distributed values between 0 and 1. For a different wavelength, λ , the induced set of phase levels still varies uniformly but does not exactly cover the range $(0, 2\pi)$:

$$\varphi(\lambda) = \frac{2\pi}{\lambda} \Delta n(\lambda) \cdot d \cdot g = \frac{\lambda_0}{\lambda} \frac{\Delta n(\lambda)}{\Delta n(\lambda_0)} \cdot \varphi(\lambda_0). \quad (2)$$

The complex modulation of a phase-only LC-SLM device, i.e., the function responsible for altering electric field going through a specific pixel, is given by

$$m(\lambda) = \exp(i\varphi(\lambda)). \quad (3)$$

Since $\varphi(\lambda_0)$ varies uniformly between 0 and 2π , $m(\lambda_0)$ corresponds to a pure exponential wave and can be used to expand $m(\lambda)$ for a different wavelength as a Fourier series [8,9]:

$$m(\lambda) = \sum_{q=-\infty}^{\infty} \eta_q m(\lambda_0)^q = \sum_{q=-\infty}^{\infty} \eta_q \exp(iq\varphi(\lambda_0)). \quad (4)$$

The coefficients of the Fourier series, η_q , defined as

$$\eta_q = \frac{1}{2\pi} \int_0^{2\pi} m(\lambda) \exp(-iq\varphi(\lambda_0)) d\varphi(\lambda_0), \quad (5)$$

can be calculated by considering Eqs. (2) and (3), and expressed using the normalized definition of the sinc function

$$\eta_q = \text{sinc} \left(\left[\frac{\lambda_0}{\lambda} \frac{\Delta n(\lambda)}{\Delta n(\lambda_0)} - q \right] \right) \cdot \exp \left(i\pi \left[\frac{\lambda_0}{\lambda} \frac{\Delta n(\lambda)}{\Delta n(\lambda_0)} - q \right] \right). \quad (6)$$

Equation (4) implies that the modulation properties of each LC-SLM pixel at wavelength λ can be expressed in terms of its modulation properties for the reference wavelength, λ_0 . As a consequence, a diffractive element obtained by 2π -wrapping at wavelength λ_0 but operating at the wavelength λ can be understood as a combination of multiple-order scaled replicas of the original refractive element. Furthermore, η_q in Eq. (6) is the complex amplitude of the q -th diffracted order and, thus, its squared modulus, $|\eta_q|^2$, produces the fraction of diffracted intensity distributed to each order. This expression correctly predicts that when $\lambda = \lambda_0$, all the energy contributes to order $q = 1$ ($\eta_q = 0, \forall q \neq 1$). Conversely, when $\lambda \neq \lambda_0$ some intensity is diverted to orders different from 1. This concept is graphically described in Fig. 2 for the case of a diffractive lens. When operating at λ_0 (top sketch) only the intended focus (first order) appears. For a different wavelength, $\lambda \neq \lambda_0$, multiple foci arise (bottom sketch). It is worth noting that, under this approach, intensity efficiency does not depend on the particular phase profile, provided that uniformly distributed phase levels are encoded in the element [8]. Thus, the chromatic response of any other diffractive optical element could be studied using this approach.

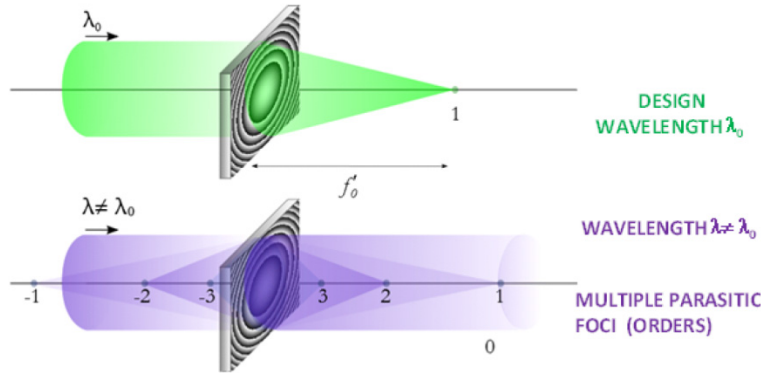


Fig. 2. Behavior of a diffractive lens when illuminated with the design wavelength (top) or a different wavelength (bottom).

For the design wavelength, λ_0 , the amplitude modulation introduced by a lens of power P_0 has a quadratic dependence on the pupil radial coordinate, r :

$$m(\lambda_0, r) = \exp\left(i \frac{\pi \cdot r^2}{\lambda_0} P_0\right). \quad (7)$$

This expression is appropriate for both a diffractive lens obtained by 2π -wrapping for this wavelength and for the original refractive spherical lens, as illustrated in Fig. 1, that could be produced if the SLM phase stroke was wide enough. However, the behavior of these two types of lenses is different for a different wavelength, λ . While a refractive lens would introduce an amplitude modulation

$$m_R(\lambda, r) = \exp\left(i \frac{\pi \cdot r^2}{\lambda} P_R(\lambda)\right), \quad (8)$$

its diffractive counterpart produces a modulation that can be expanded as a Fourier series using the formalism leading to Eq. (4),

$$m_D(\lambda, r) = \sum_{q=-\infty}^{\infty} \eta_q m(\lambda_0, r)^q = \sum_{q=-\infty}^{\infty} \eta_q \exp\left(i \frac{\pi \cdot r^2}{\lambda_0} q P_0\right) = \sum_{q=-\infty}^{\infty} \eta_q \exp\left(i \frac{\pi \cdot r^2}{\lambda} P_{D,q}(\lambda)\right). \quad (9)$$

The expression in Eq. (8) corresponds to a monofocal lens whose power, considering the relationship between $\varphi(\lambda)$ and $\varphi(\lambda_0)$ in Eq. (2), is

$$P_R(\lambda) = \frac{\Delta n(\lambda)}{\Delta n(\lambda_0)} \cdot P_0. \quad (10)$$

This relationship is analogous to the typical longitudinal chromatic aberration in refractive lenses due to chromatic dispersion. Instead, the diffractive profile in Eq. (9) behaves as a multifocal lens, with optical power, for the q -th focal point,

$$P_{D,q}(\lambda) = q \cdot \frac{\lambda}{\lambda_0} \cdot P_0. \quad (11)$$

Interestingly, this expression of the power sequence only depends on the wavelength ratio, as befits a diffractive element, and the focal-point order, q , but not on liquid crystal chromatic dispersion, $\Delta n(\lambda)/\Delta n(\lambda_0)$, which only affects intensity allotment among orders (see Eq. (5)).

Figure 3(a) represents the normalized intensity efficiency of diffraction order q from -5 to 5 , for different wavelengths, which approximately cover the visible range. It should be noted that only integer values of q , represented by symbols, exist, but continuous lines are included in order to help visualization. The relative index dispersion, $\Delta n(\lambda)/\Delta n(\lambda_0)$, of the SLM is required to obtain these values. This parameter may be obtained indirectly from the technical specifications of the LC-SLM. Instead, in this work it was experimentally obtained as described in another section below.

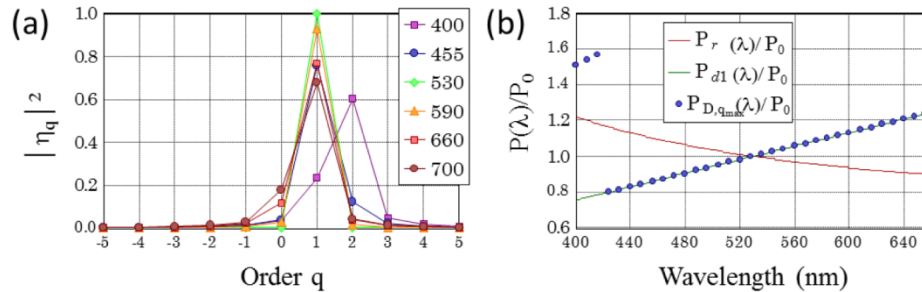


Fig. 3. (a) Intensity efficiency vs. diffraction order, q , for different wavelengths in the visible range. (b) Optical power dispersion curves for a refractive lens (red solid curve) together with the first diffraction order (solid green curve) and the overall predominant dispersion (blue circles) of the corresponding diffractive lens.

From Fig. 3(a), the amplitude corresponding to the reference wavelength, $\lambda_0 = 532$ nm in our case, is zero at any diffraction order different from 1 as would correspond to a theoretically perfect response of the LC-SLM. For other wavelengths, the amplitude of order 1 decreases and some of the available energy is redirected to other parasitic orders. Except for the shortest wavelength considered, order 1 remains the most intense, being the others significantly dimmer in terms of energy. For the particular case of 400 nm, order $q = 2$ receives more intensity than order 1. In general, the intensity removed from $q = 1$ for wavelengths $\lambda \neq \lambda_0$ is spread among other orders, predominantly towards $q = 2$ for $\lambda < \lambda_0$ and towards $q = 0$ for $\lambda > \lambda_0$.

In order to illustrate the behavior of lens power with wavelength, Fig. 3(b) shows the chromatic power factor, i.e., the ratio between power for wavelength λ and for the reference wavelength, $P(\lambda)/P_0$. For each diffractive order, the power factor is proportional to the ratio between wavelengths and, accordingly, increases towards red and decreases towards blue. Green lines represent the power factor for diffractive orders $q = 1$ (solid) and $q = 2$ (dashed), that are the relevant orders when using a reference wavelength around the center of the visible

spectrum, as evidenced by the intensity distribution shown in Fig. 3(a). For most of the visible spectrum, the most intense diffractive order is $q = 1$, but for short wavelengths it declines in favor of $q = 2$. Defining the effective focal point of the lens as that point with the maximum intensity concentration, the effective power factor (blue symbols in Fig. 3(b)) switches from $q = 1$ to $q = 2$ around 420 nm. This transition wavelength is related to the design wavelength and can be pushed outside the visible by selecting a shorter λ_0 . For comparison purposes, Fig. 3(b) also shows the power factor for a refractive profile, which equals the ratio between refractive indexes (see Eq. (10)) and was experimentally determined as described in a later section for a commercially available SLM model. Predictably, the chromatic behavior follows opposite trends for refractive and diffractive lenses.

3. Experiments

The chromatic model described in the previous section was experimentally tested using a LC-SLM (Pluto VIS, Holoeye Photonics AG, Germany). The LC-SLM was calibrated following a protocol described elsewhere [12]. The procedure was repeated for four wavelengths, three of them obtained by means of a high-power polychromatic LED light source (LED4D202, Thorlabs Inc, USA) coupled to interchangeable narrow-band interferential filters (centered at 450 nm, 550 nm and 650 nm), and a fourth wavelength (532 nm) from a diode laser (CPS532, Thorlabs Inc, USA). The latter was used as the reference wavelength. The phase calibration results for each wavelength are presented in Fig. 4(a).

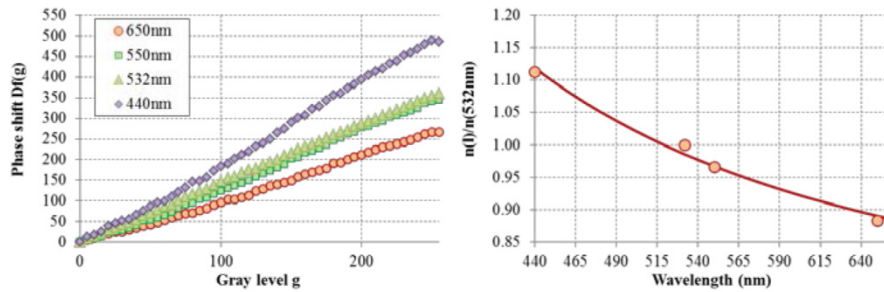


Fig. 4. (a) Phase calibration curves for the tested wavelengths. (b) Experimental refractive index ratio for each wavelength (symbols) and Cauchy-like fitting curve (red line). Reference wavelength $\lambda_0 = 532$ nm.

The slope of each curve in Fig. 4(a) is related to the effective index range, $\Delta n(\lambda)$, for the corresponding wavelength. The relative index dispersion can be estimated from the slope, $a(\lambda)$, of these curves, obtained by linear fitting:

$$\frac{\Delta n(\lambda)}{\Delta n(\lambda_0)} \cong \frac{a(\lambda) \cdot \lambda}{a(\lambda_0) \cdot \lambda_0}. \quad (12)$$

The symbols in Fig. 4(b) represent the experimental index ratio for each wavelength. These data can be fitted to a Cauchy dispersion model. The obtained dispersion equation was:

$$\frac{\Delta n(\lambda)}{\Delta n(\lambda_0)} \cong 0.6985 + \frac{8.125 \cdot 10^4}{\lambda^2} + \frac{8.292 \cdot 10^5}{\lambda^4}, \quad (13)$$

with λ expressed in nm. The numerical values in Eq. (13) are specific of the tested SLM. This expression was used in Fig. 3(b).

To experimentally verify the chromatic model, the point spread functions (PSFs) associated to a phase profile produced on the LC-SLM were recorded for different wavelengths by using the experimental setup schematized in Fig. 5. The polychromatic LED source combines 4 narrow-band LEDs. The emitting wavelengths for model LED4D202 are

455 nm, 530 nm, 590 nm, and 660 nm (FWHM = 20 nm, 31 nm, 15 nm, and 17 nm, respectively). The light emerging from the source was spatially filtered by a microscope objective (OBJ) and a pinhole (PH), and collimated by achromatic lens L_c . A linear polarizer P selected the appropriated polarization for the SLM to operate under pure phase modulation. The radius of the input pupil (IP) was $\rho = 4.5$ mm. Two 1:1-magnification telescopes, composed of lens pairs L_1 - L_2 and L_3 - L_4 , conjugated the SLM plane with P1 and P2 planes. Lens L_7 (200 mm focal length) was placed on the P2 plane and generated the PSF for the induced phase profile onto the camera (Manta G125B, Allied Vision Technologies GmbH, Germany).

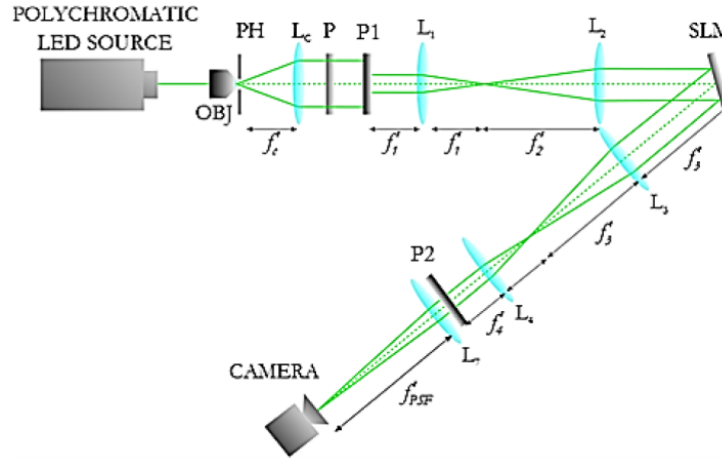


Fig. 5. Experimental setup used for obtaining the spectral response of a phase profile programmed into the SLM. Legend: OBJ, microscope objective; PH, pinhole aperture; L_c , collimating lens; P, polarizer; P1 and P2, conjugated pupil planes; L_1 - L_2 and L_3 - L_4 , relay telescopes; and L_7 , PSF-generating lens.

The phase profile corresponding to a 1-diopter lens 2π -wrapped for a reference wavelength of 532 nm was programmed into the LC-SLM and the PSF was sequentially recorded for each individual wavelength at the LED source. Since the PSF-forming lens was in the P2 plane, the power, $P(\lambda)$, induced by the phase profile in the LC-SLM directly adds to the lens power, P_{PSF} . Neglecting misalignments and additional aberrations, simple geometrical optics predicts a diameter for the PSF that is proportional to the phase profile power, which is a function of wavelength:

$$\varnothing_{PSF} = 2\rho \cdot \frac{P(\lambda)}{P_{PSF}}, \quad (14)$$

where ρ is the radius of the exit pupil. This expression can be used to estimate the PSF diameter for a refractive profile. For the 2π -wrapped profile, it predicts the diameter for each diffractive order individually. The combined PSF diameter can be expected to be similar to that of the most intense diffraction order, except for the transition between orders, when two of them have similar intensities (around 420 nm in our case).

Figure 6(a) shows the experimental PSF diameter (circles), measured as the distance between the most external lobes, as a function of wavelength, together with the theoretical values (triangles) predicted by using Eq. (14) in combination with Eq. (11) for $q = 1$, which is the most intense diffractive order for the four wavelengths considered. In order to avoid small scaling errors, both curves were matched for the reference wavelength, 532 nm.

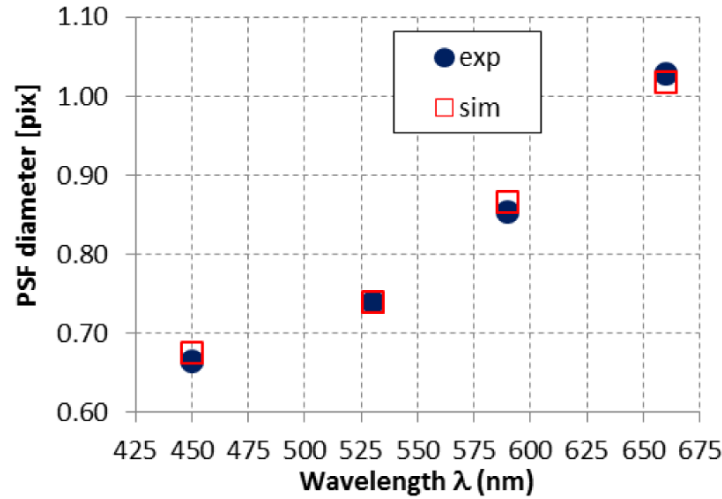


Fig. 6. Theoretical (squares) and experimentally determined (circles) diameter of the PSF corresponding to a 1D lens 2π -wrapped for 532 nm.

4. Application to correct the eye's chromatic aberration

As an example of application, we studied the interaction of a diffractive lens generated in the SLM with the longitudinal chromatic aberration of a human eye. Atchison and Smith [13] provide an expression in the form of a Cauchy expansion for the eye's chromatic difference of refraction with respect to 590 nm. For this example, we shifted the reference point to 550 nm, which is close to the maximum eye's sensitivity, and reversed the sign to obtain the difference in power, $D_{eye}(\lambda)$. The resulting expression is

$$D_{eye}(\lambda) = -1.81341 + \frac{6.70941 \cdot 10^5}{\lambda^2} - \frac{5.5534 \cdot 10^{10}}{\lambda^4} + \frac{5.59998 \cdot 10^{15}}{\lambda^6}. \quad (15)$$

From Eq. (11) and considering the 1st diffraction order, $q = 1$, the longitudinal chromatic aberration induced by the SLM when programming a diffractive lens of power P_0 2π -wrapped for the same wavelength is

$$D_{SLM}(\lambda) = P_0 \left[\frac{\lambda}{\lambda_0} - 1 \right]. \quad (16)$$

When using 550 nm as the reference wavelength, the transition from $q = 1$ to $q = 2$ as the most intense diffraction order occurs around 425 nm. Therefore, Eq. (16) is valid for most of the visible spectrum.

For positive values of P_0 , Eqs. (15) and (16) have opposite tendencies with wavelengths. Therefore, a positive diffractive lens partially compensates the eye's longitudinal chromatic aberration. In particular, if the eye sees through a positive 3.2D lens implemented in the LC-SLM as a diffractive profile 2π -wrapped for 550 nm, the chromatic difference of power for the combination is at its minimum and almost flat in the range from 450 nm to 700 nm, as illustrated in Fig. 7. That sort of arrangement could be used to study vision after longitudinal chromatic aberration correction, provided the overall focus error was corrected by an achromatic lens.

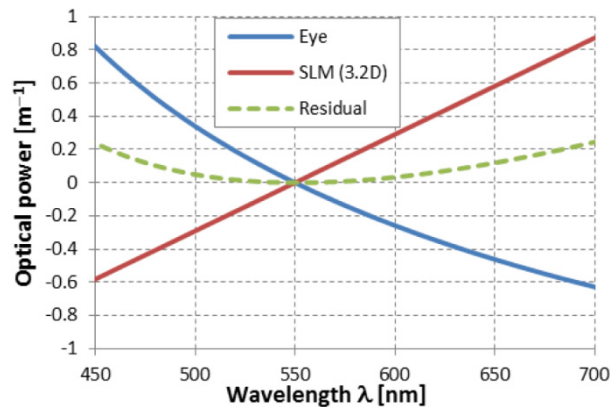


Fig. 7. Power dispersion for the naked eye (blue), for a 3.2D diffractive lens generated with the SLM (red), and for the combination of both (green).

5. Conclusions

We used Fourier series analysis to study the chromatic effects of a phase wrapped profile when used for a wavelength that is different from the design wavelength. This produces the generation of multiple scaled diffractive replicas of the intended phase profile, although typically only one of them has a relevant light intensity concentration. We presented a model for describing the dispersion exhibited by lenses and other phase profiles implemented in an LC-SLM as diffractive elements by 2π -wrapping at a reference wavelength. It has been derived that first diffraction order concentrates most of the diffracted energy for the visible range, and that dispersion is linear with wavelength. Experimental tests for this behavior have been provided. As an example of potential application, the model has been used to study the coupling of a diffractive lens with the chromatic aberration of the human eye. Positive lenses partially compensate the eye's chromatic difference in defocus, with the best compensation found for a 3.2D lens. This approach may offer a practical approach for the accurate correction of chromatic defocus differences in a variety of experiments and applications.

Funding

European Research Council Advanced Grant (ERC-2013-AdG-339228, SEECAT); Secretaría de Estado e Investigación, Desarrollo e Innovación-SEIDI (FIS2016-76163-R); Fundación Séneca-Agencia de Ciencia y Tecnología de la Región de Murcia (grants 18964/JLI/13 and 19897/GERM/15); European Regional Development Fund (EU-FEDER) and VALID fellowship to J.L. Fuentes.